Suspended optical fiber-to-waveguide mode size converter for Silicon photonics

Qing Fang[1]*, Tsung-Yang Liow[1], Jun Feng Song[1, 2], Chee Wei Tan[1], Ming Bin Yu[1], Guo Qiang Lo[1] and Dim-Lee Kwong[1]

[1]*Institute of Microelectronics, A*STAR (Agency for Science, Technology and Research), 11 Science Park Road, Singapore Science Park II, Singapore 117685.*

[2]*State Key Laboratory on Integrated opto-electronics, College of Electronic Science and Engineering, Jilin University, Changchun, People's Republic of China, 130023*

**Fangq@ime.a-star.edu.sg*

Abstract: In this paper, an efficient and novel optical fiber-to-waveguide mode size converter for Si Photonics devices with sub-micron waveguides is developed on the SOI platform. This optical converter is composed of a suspended SiO_2 waveguide and overlapped Si nano-tapers located in the center of suspended SiO_2 waveguide. Laterally connected SiO_2 beams provide structural support for the suspended SiO_2 waveguide. The optical input signal from the optical fiber is launched into the suspended SiO_2 waveguide, and then coupled into the Si nano-taper. The measured coupling loss using a lensed fiber with 5 μm spot diameter is 1.7 ~2.0 dB/facet for TE mode and 2.0 ~2.4 dB/facet for TM mode in the wavelength range of 1520 ~1600 nm. When a cleaved fiber with 9.2μm spot diameter is used, the coupling losses for both TE and TM modes are less than 4.0 dB/facet at 1550 nm. For the case of lensed fiber, the alignment tolerances for both TE and TM modes are about ± 1.7 μm for 1 dB excess loss in both X and Y axes. The alignment tolerances for both modes of TE and TM are relaxed, exceeding ± 2.5 μm for 1 dB excess loss in both X and Y axes when a cleaved fiber is used.

OCIS Codes: (130.3120) Integrated optics devices; (130.2790) Guided waves; (220.0220) Optical design and fabrication; (220.4000) Microstructure fabrication; (230.3990) Microstructure devices

References and links:

1. P. Dumon, W. Bogaerts, V. Wiaux, J. Wouters, S. Beckx, J. Van Campenhout, D. Taillaert, B. Luyssaert, P. Bienstman, D. Van Thourhout, and R. Baets, "Low-loss SOI photonic wires and ring resonators fabricated with deep UV lithography," IEEE Photon. Technol. Lett. **16**(5), 1328–1330 (2004).
2. W. Bogaerts, P. Dumon, D. V. Thourhout, D. Taillaert, P. Jaenen, J. Wouters, S. Beckx, V. Wiaux, and G. R. Baets, "Compact wavelength-selective functions in Silicon-on-Insulator photonic wires," IEEE J. Sel. Top. Quantum Electron. **12**(6), 1394–1401 (2006).
3. Q. Fang, J. F. Song, S. H. Tao, M. B. Yu, G. Q. Lo, and D. L. Kwong, "Low loss (~ 6.45 dB/cm) sub-micro polycrystalline silicon waveguide integrated with efficient SiON waveguide coupler," Opt. Express **16**(9), 6425–6432 (2008).
4. A. Liu, R. Jones, L. Liao, D. Samara-Rubio, D. Rubin, O. Cohen, R. Nicolaescu, and M. Paniccia, "A high-speed silicon optical modulator based on a metal-oxide-semiconductor capacitor," Nature **427**(6975), 615–618 (2004).
5. A. Liu, L. Liao, D. Rubin, H. Nguyen, B. Ciftcioglu, Y. Chetrit, N. Izhaky, and M. Paniccia, "High-speed optical modulation based on carrier depletion in a silicon waveguide," Opt. Express **15**(2), 660–668 (2007).
6. Q. Xu, B. Schmidt, S. Pradhan, and M. Lipson, "Micrometre-scale silicon electro-optic modulator," Nature **435**(7040), 325–327 (2005).
7. J. B. You, M. Park, J. W. Park, and G. Kim, "12.5 Gbps optical modulation of silicon racetrack resonator based on carrier-depletion in asymmetric p-n diode," Opt. Express **16**(22), 18340–18344 (2008).
8. T. Y. Liow, K. W. Ang, Q. Fang, J. F. Song, Y. Z. Xiong, M. B. Yu, G. Q. Lo, and D. L. Kwong, "Silicon Modulators and Germanium Photodetectors on SOI: Monolithic Integration, Compatibility and Performance Optimization," IEEE J. Sel. Top. Quantum Electron. (Article In Press).
9. T. Yin, R. Cohen, M. M. Morse, G. Sarid, Y. Chetrit, D. Rubin, and M. J. Paniccia, "31 GHz Ge n-i-p waveguide photodetectors on Silicon-on-Insulator substrate," Opt. Express **15**(21), 13965–13971 (2007).

#122312 - $15.00 USD Received 6 Jan 2010; revised 25 Feb 2010; accepted 26 Feb 2010; published 30 Mar 2010

10. L. Chen, and M. Lipson, "Ultra-low capacitance and high speed germanium photodetectors on silicon," Opt. Express **17**(10), 7901–7906 (2009).
11. D. Ahn, C. Y. Hong, J. F. Liu, W. Giziewicz, M. Beals, L. C. Kimerling, J. Michel, J. Chen, and F. X. Kärtner, "High performance, waveguide integrated Ge photodetectors," Opt. Express **15**(7), 3916–3921 (2007).
12. H. Rong, R. Jones, A. Liu, O. Cohen, D. Hak, A. Fang, and M. Paniccia, "A continuous-wave Raman silicon laser," Nature **433**(7027), 725–728 (2005).
13. H. Rong, A. Liu, R. Jones, O. Cohen, D. Hak, R. Nicolaescu, A. Fang, and M. Paniccia, "An all-silicon Raman laser," Nature **433**(7023), 292–294 (2005).
14. O. Boyraz, and B. Jalali, "Demonstration of a silicon Raman laser," Opt. Express **14**, 4261–4268 (2004).
15. J. F. Song, Q. Fang, S. H. Tao, T. Y. Liow, M. B. Yu, G. Q. Lo, and D. L. Kwong, "Fast and low power Michelson interferometer thermo-optical switch on SOI," Opt. Express **16**(20), 15304–15311 (2008).
16. Q. Fang, J. F. Song, G. Zhang, M. B. Yu, Y. L. Liu, G. Q. Lo, and D. L. Kwong, "Monolithic integration of a multiplexer/demultiplexer with a thermo-optic VOA array on an SOI platform," IEEE Photon. Technol. Lett. **21**(5), 319–321 (2009).
17. H. Yamada, T. Chu, S. Ishida, and Y. Arakawa, "Si photonic wire waveguide devices," IEEE J. Sel. Top. Quantum Electron. **12**(6), 1371–1379 (2006).
18. V. R. Almeida, R. R. Panepucci, and M. Lipson, "Nanotaper for compact mode conversion," Opt. Lett. **28**(15), 1302–1304 (2003).
19. T. Shoji, T. Tsuchizawa, T. Watanabe, K. Yamada, and H. Morita, "Low loss mode size converter from 0.3 μm square Si wire waveguides to singlemode fibers," Electron. Lett. **38**(25), 1669–1670 (2002).
20. T. Tsuchizawa, K. Yamada, H. Fukuda, T. Watanabe, J. Takahashi, M. Takahashi, T. Shoji, E. Tamechika, S. Itabashi, and H. Morita, "Microphotonics devices based on silicon microfabrication technology," IEEE J. Sel. Top. Quantum Electron. **11**(1), 232–240 (2005).
21. F. Van Laere, T. Claes, J. Schrauwen, S. Scheerlinck, W. Bogaerts, D. Taillaert, L. O'Faolain, D. Van Thourhout, and R. Baets, "Compact focusing grating couplers for Silicon-on-Insulator integrated circuits," IEEE Photon. Technol. Lett. **19**(23), 1919–1921 (2007).
22. F. Van Laere, G. Roelkens, M. Ayre, J. Schrauwen, D. Taillaert, D. Van Thourhout, T. F. Krauss, and R. Baets, "Compact and highly efficient grating couplers between optical fiber and nanophotonic waveguides," J. Lightwave Technol. **25**(1), 151–156 (2007).
23. B. Analui, D. Guckenberger, D. Kucharski, and A. Narasimha, "A fully integrated 20-Gb/s optoelectronic transceiver implemented in a standard 0.13-μm CMOS SOI technology," IEEE J. Solid-state Circuits **41**(12), 2945–2955 (2006).

1. Introduction

Silicon photonics devices based on Silicon-on-Insulation (SOI) have become an active research and development field, due to the high refractive index contrast between the silicon core and the oxide cladding. The high refractive index contrast enables high-density integrated optical circuits, which can be fabricated by standard complementary metal-oxide-semiconductor (CMOS) technology. It is possible to realize mass production and reduce the cost effectively. In the past decade, silicon photonic has been attracting to many research groups in the world and many optical SOI components have been demonstrated, including compact and low loss SOI passive waveguide devices [1–3], high speed silicon modulator [4–8], high speed GeSi modulator [9–11], silicon Raman lasers [12–14] and other thermo-optic devices [15,16]. Although silicon photonics devices on SOI platform have many advantages and have been widely developed, there is a disadvantage for silicon photonics devices' application. The waveguide dimension of silicon photonics device is very small, only several hundreds of nanometers. Thus, there is a mode size mismatch between the nano-scale Si waveguide and the single mode fiber (SMF). The coupling loss is very high if the nano-scale silicon waveguide directly couples with the single mode fiber. At the same time, the alignment tolerance is small; and it is a challenge to package silicon photonics devices with single mode fiber. So, the optical mode size converter between the single mode fiber and nano-scale Si waveguide is a vital component for all of silicon photonics devices.

Some important research works have contributed to the development of low loss optical mode size converter for silicon photonic devices. The simplest structure is Si nano-tip covered with a low refractive index SiO_2 layer [17,18]. This converter has 2.0 ~3.0 dB/facet coupling loss with a tapered fiber. This kind of converter is an excellent characterization solution with the tapered fiber for silicon photonic devices; however, it is difficult to be packaged because of the tight alignment tolerance. A low loss polymer converter has been demonstrated by NTT [19]. The polymer covers the nano-scale Si tip and the coupling loss to optical fiber is about 0.8 dB/facet. However, the process is not compatible with CMOS technology. Later, NTT

#122312 - $15.00 USD Received 6 Jan 2010; revised 25 Feb 2010; accepted 26 Feb 2010; published 30 Mar 2010

fabricated the same converter using SiON material as the cladding waveguide and the coupling loss is about 2.5 dB/facet [20]. Another important converter is the vertical grating coupler [21–23]. The vertical grating coupler has a flex alignment tolerance; however, it is a wavelength dependent device.

In this work, we designed and fabricated an efficient and novel optical fiber-to-waveguide mode size converter for Si Photonics devices based on nano-scale waveguides on the SOI platform. It is almost wavelength independent. It is composed of a suspended SiO_2 waveguide and an overlapped Si nano-taper located in the center of the suspended SiO_2 waveguide. In order to strengthen the suspended SiO_2 waveguide, narrow SiO_2 beams were fabricated to connect the suspended SiO_2 waveguide to the deposited SiO_2 layer. If compared to previous converters, the process is very simple and easy to control. At the same time, this converter provides a good solution to package with the optical fiber.

2. Design and fabrication

As we know, the optical single mode fiber is made of the SiO_2 material. Compared to other materials, the major advantage of SiO_2 converter is the improvement in transmission and reduction in return loss from optical fiber to converter. In order to confine the optical mode within the SiO_2 waveguide, it is necessary to etch and isolate the SiO_2 waveguide from the Si substrate, so as to form a suspended SiO_2 waveguide.

Figure 1shows the schematic diagram of our converter. It is composed of a suspended SiO_2 waveguide and a Si nano-taper. In order to compress the mode size in the vertical direction (Y axis), a partial etch of SiO_2 is used to create a ridge on top of the SiO_2 waveguide which tapers laterally down to a minimum width of 300 nm at its termination, forming a terminated taper. The suspended SiO_2 waveguide is also laterally tapered such that the dimensions are larger at the input facet and smaller at the Si taper. This lateral taper serves to compress the input optical mode size to match the Si nano-taper mode size in the horizontal direction (X axis).

A lateral Si nano-taper is used to match the optical mode of the SiO_2 waveguide in the horizontal direction. At the same time, in order to enlarge the vertical optical mode size of the Si nano-taper to match the mode of the SiO_2 waveguide, an overlapped Si nano-taper is employed. The optical signal from the optical fiber is first coupled into the suspended SiO_2 waveguide. Then, the optical signal propagates in the suspended SiO_2 waveguide and is laterally and vertically compressed by the SiO_2 lateral taper and the SiO_2 terminated taper, respectively. Then, the optical signal is coupled into the overlapped Si nano-taper, and finally into the Si waveguide.

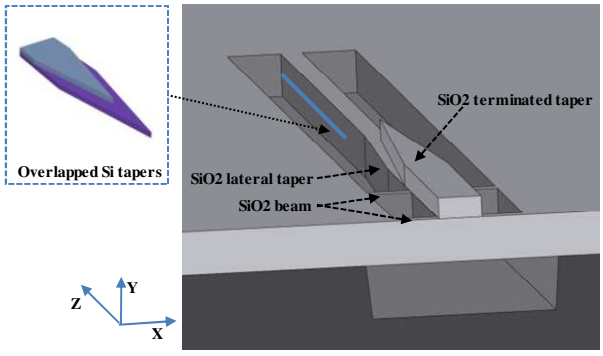

Fig. 1. Schematic diagram of suspended converter; inset: Overlapped Si tapers

The suspended SiO_2 waveguide is 6 μm × 6 μm in cross-section at the input end. Laterally, it tapers down from 6 μm to 2 μm in width along a 60 μm-long section. The overlapped Si nano-tapers are located in the narrow SiO_2 waveguide and have a 5 μm distance from the end of the above-mentioned lateral taper. The gap between the SiO_2 waveguide and the adjacent SiO_2 layer of 2 μm is to avoid the optical signal leakage into the adjacent SiO_2 layer. Also, in

#122312 - $15.00 USD Received 6 Jan 2010; revised 25 Feb 2010; accepted 26 Feb 2010; published 30 Mar 2010

order to avoid the optical signal leakage into the Si substrate, the gap between the SiO_2 waveguide and Si substrate is more than 2 μm. Another SiO_2 terminated taper with a 300 nm-wide tip is designed on the lateral taper. It is 1 μm thick and 50 μm long. SOI wafers with 220 nm top Si layer and 2 μm buried oxide (BOX) was used. As such, the overlapped Si nano-taper is near the center of suspended SiO_2 waveguide, allowing for optimal coupling efficiency between the suspended SiO_2 waveguide and the Si nano-taper. The overlapped tapers are shown in Fig. 1(inset). The two Si tapers have the same lengths and widths; but have different thicknesses. The designed top Si taper is 150 nm wide and 140 nm thick. The suspended SiO_2 waveguide is about 150 um long. In order to provide the support for the suspended SiO_2 waveguide, 2 pairs of SiO_2 beams are designed, as shown in Fig. 1. The length of the beam is only 1 μm along the propagation direction to minimize the optical crossing loss. The designed dimension of Si waveguide connect with the overlapped Si nano-taper is 220 nm (thickness) × 500 nm (width). The tip width of the Si nano-taper is critical for the coupling loss. In fact, the optical loss caused by the beam can be negligible. So, in the simulation, the structure is without the narrow beams. The suspended structure is simulated using the beam propagation method (BPM) of RSOFT software, shown in Fig. 2. The input fiber mode field diameter is 6 μm. Figure 2(a) is the mode field distribution with the 30 nm wide Si tip and it shows coupling efficiency is very good. Figure 2(b) is the coupling loss per facet vs. tip width of Si nano-taper and it shows that a coupling efficiency of up to 82% (~0.9 dB/facet) can be obtained for TE mode at a wavelength of 1.55 um when the tip width is 30 nm. Due to the limitation of our process, we fabricated the Si taper with a 110nm-wide tip, which corresponds to a simulated coupling loss of about 1.4 dB/facet.

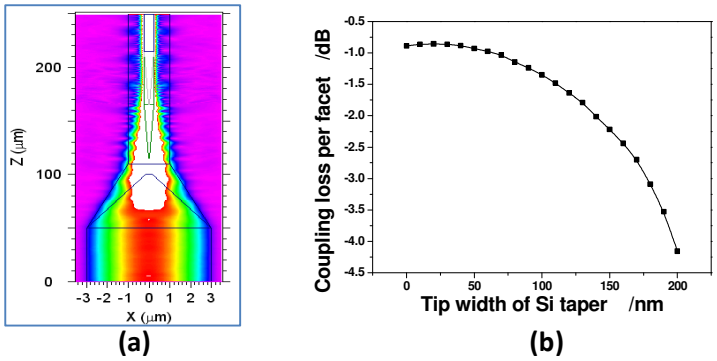

Fig. 2. Simulation results of suspended converter at 1550 nm for TE mode: (a) Mode field distribution (Z axis is the propagation direction); (b) coupling loss per facet vs. tip width of Si nano-taper

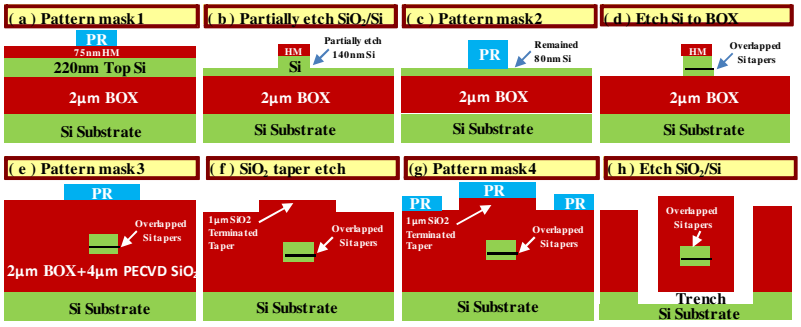

Fig. 3. Fabrication process flow chart for optical converter

In our experiment, a 200 mm-diameter Si wafer with 220 nm top Si and 2 μm BOX was used. The process flow chart is shown in Fig. 3. After 75 nm PECVD SiO_2 deposition as the

#122312 - $15.00 USD Received 6 Jan 2010; revised 25 Feb 2010; accepted 26 Feb 2010; published 30 Mar 2010

hard mask (HM), the waveguide and top taper structures are patterned using 248 nm deep UV lithography technology, as shown in Fig. 3(a). The photo-resist (PR) pattern size is closed to the design value. Then, the PR pattern is trimmed using O_2 gas before etching the SiO_2 hard mask. After trimming, the tip width of the taper and the waveguide width become 110 nm and 450 nm, respectively. The SiO_2 hard mask is then opened using carbon tetrafluoride (CF_4) and 140 nm Si is partially etched using chlorine (Cl_2) and oxygen, as shown in Fig. 3(b). The formation of top Si nano-taper is completed by the first partially Si etching. In order to form the bottom Si nano-taper, the wafer is patterned and trimmed again; and then, the remained 80 nm Si is etched using Cl_2, shown as in Fig. 3(c), 3(d). After this process, the overlapped Si nano-taper and Si waveguide is formed. In Fig. 4(a), 4(b), the scanning electron microscope (SEM) images of overlapped Si nano-taper are shown. The left SME image is the bottom Si nano-taper on the BOX; and the right SME image is the top Si nano-taper on a slab waveguide which is the same layer with the bottom Si nano-taper. After formation of overlapped Si nano-tapers, a 4 μm PECVD SiO_2 layer is deposited. So, the SiO_2 surrounds the Si waveguide. Then, the 1 μm-thick SiO_2 terminated taper is patterned and etched, as shown in Fig. 3(e), 3(f). Its SEM image is shown in Fig. 4(c). Later, the SiO_2 waveguide and deep trench are patterned, as shown in Fig. 3(g). After patterning, the SiO_2 layer is etched by octofluorocyclobutane (C_4F_8); and Si layer is etched by sulfur fluoride (SF_6) to form the suspended SiO_2 waveguide and Si deep trench, as shown in Fig. 3(h). The processed suspended converter is shown in Fig. 4(d). Figure 4(e) is the input port of the suspended converter. The deep trench process eliminates the need for mechanical polishing prior to optical measurements. Finally, the processed wafer is diced for measurement. In order to get the coupling loss of the suspended converter, we design the cut-back structures, including 5 Si waveguides (WG1~WG5) with the same suspended converters at the input/output ports. All of cut-back structures have the same dimension and the same bend waveguides. The diameter of bend waveguides is 20 μm, so the bend loss can be negligible. The lengths of WG1~WG5 are 4.06 mm, 8.06 mm, 12.06 mm, 16.06 mm and 20.06 mm, respectively.

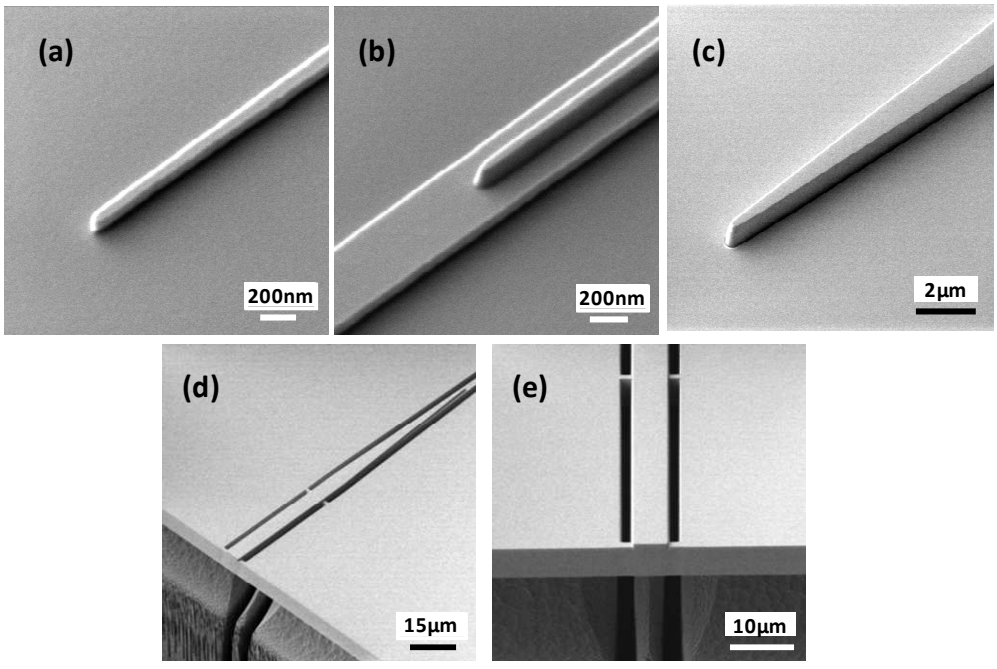

Fig. 4. SEM images of the suspended converter: (a) Bottom Si taper; (b) Top Si taper; (c) SiO_2 terminated taper; (d) Suspended converter; (e) Input port of suspended converter.

#122312 - $15.00 USD Received 6 Jan 2010; revised 25 Feb 2010; accepted 26 Feb 2010; published 30 Mar 2010

3. Results and analysis

The coupling loss of the converter can be characterized by the cut-back method using a high-precision tunable light source with broad band wavelengths, a polarization controller, a polarizer and an optical high-precision power meter. First, we used two lensed optical polarization-maintaining (PM) fibers (mode spot diameter ~5 μm) to couple the Si cut-back waveguides with input/output mode size converters. In order to measure the insertion loss of TE/TM mode, we adjust the polarization controller and rotate the PMF holder before testing the waveguides.

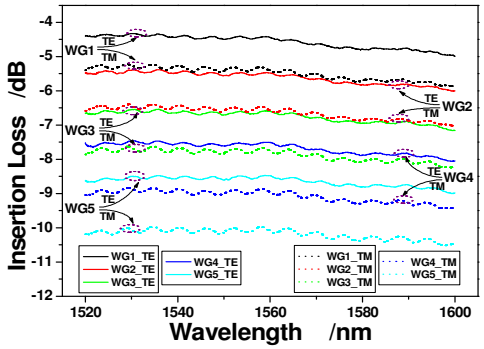

Fig. 5. Insertion loss of cut-back waveguides for TE/TM mode measured with 5 μm spot diameter lensed fibers

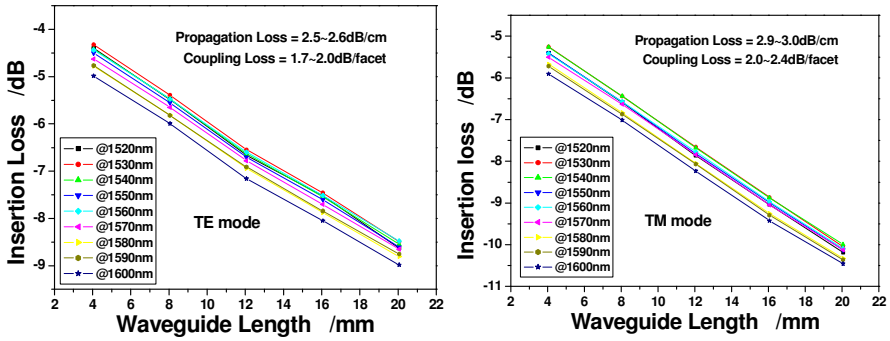

(a) TE mode (b) TM mode

Fig. 6. Coupling loss and propagation loss for TE/TM mode using 5 μm spot diameter lensed fibers

The measured insertion loss of TE/TM mode is shown in Fig. 5. According to these spectra of insertion loss, we can calculate the coupling loss and propagation loss at different wavelengths, as shown in Fig. 6. At the wavelength range of 1520 ~1600 nm, the coupling loss and propagation loss is 1.7 ~2.0 dB/facet and 2.5 ~2.6dB/cm for TE mode, respectively; and, 2.0 ~2.4 dB/facet and 2.9 ~3.0 dB/cm for TM mode, respectively. We also measured the coupling loss using the cleaved fiber with a 9.2 μm mode spot diameter at 1550 nm. The coupling loss at 1550nm is 3.8 dB/facet for TE mode and 4.0 dB/facet for TM mode, as shown in Fig. 7.

The alignment tolerance of the optical converter is a very critical parameter for the fiber assembly. Hence, the tolerances of our converter in both X and Y axes at 1550 nm are characterized. From the above results of cut-back structures, the propagation loss of Si waveguide is 2.5 dB/cm for TE mode and 2.9 dB/cm for TM mode. The total propagation loss of Si waveguide is decoupled from the measured insertion loss; and the measured alignment tolerances are shown in Fig. 7. For the lensed fiber with a 5 μm mode spot diameter, the

#122312 - $15.00 USD Received 6 Jan 2010; revised 25 Feb 2010; accepted 26 Feb 2010; published 30 Mar 2010

alignment tolerances in both X and Y axes are ± 1.7 μm for 1dB excess loss. For the case of cleaved fiber with 9.2 μm mode spot diameter, the alignment tolerances in both X and Y axes exceed ± 2.5 μm for 1dB excess loss. We also used the lensed fibers and cleaved fibers to couple with the Si nano-tip only covered by the SiO_2 cladding, similar to the structure reported in reference [17]. Without the suspended structure, the coupling loss of Si nano-taper is 2.5 ~3.0 dB/facet using the lensed PM fiber for both TE and TM modes, with an alignment tolerance of less than ± 1 μm for 1 dB excess loss. It also shows that the coupling loss of the nano-taper coupled with cleaved fibers is very high (~8 dB/facet) for both TE and TM modes. So, this suspended converter can improve the alignment tolerance and reduce the coupling loss.

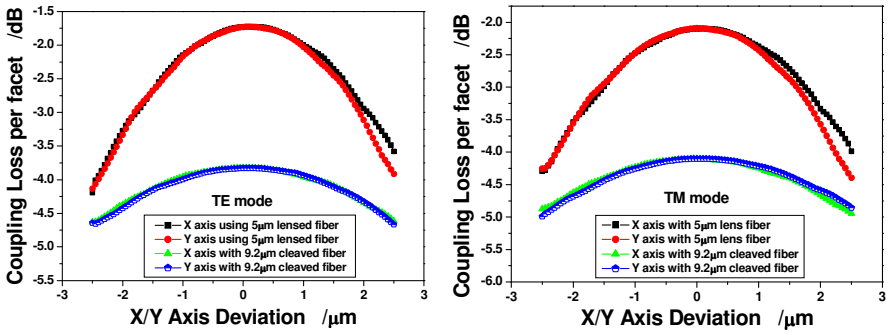

Fig. 7. Alignment tolerances of the suspended converter for both X and Y axes at 1550 nm

4. Conclusion

An efficient and novel optical fiber-to-waveguide mode size converter for Si Photonics devices has been presented in this paper. This converter is composed of the suspended SiO_2 waveguide and the overlapped Si nano-taper. The measured results show coupling loss of the converter coupled with the lensed fibers is 1.7 ~2.0 dB/facet for TE mode and 2.0 ~2.4 dB/facet for TM mode in the broad wavelength range of 1520 ~1600 nm. The alignment tolerance is ± 1.7 μm for 1dB excess loss in both X and Y axes at 1550 nm. For the case of the cleaved fiber with 9.2 μm mode spot diameter, the coupling loss is less than 4.0 dB/facet for TE/TM mode; and the alignment tolerance exceeds ± 2.5 μm for 1dB excess loss. The converter can be further optimized to reduce the coupling loss with the cleaved fiber by increasing the dimension of the input SiO_2 waveguide in X and Y axes. It would be a useful component to improve the coupling efficiency in the fiber attachment process.

#122312 - $15.00 USD Received 6 Jan 2010; revised 25 Feb 2010; accepted 26 Feb 2010; published 30 Mar 2010